# High Accuracy Real-time Dam Monitoring Using Low-cost GPS Equipment

**Reda ALI, Paul CROSS, United Kingdom and Ali EL-SHARKAWY, Egypt**

**Key words**: Multipath, Sidereal-day correction, Pacoima Dam, GPSEM .

## SUMMARY

A methodology for GPS engineering monitoring using GPS (GPSEM) has been developed and implemented in a software package at the Department of Geomatic Engineering, University College London (UCL). It detects the movements occurring in engineering objects by applying the sidereal-day correction technique for phase GPS multipath errors, a Kalman filter and a Cumulative SUM (CUSUM) control chart. In order to meet the objective of providing a low-cost system, the method uses only L1 phase observables to detect and quantify these movements. After promising success of the system and software on a controlled experiments were conducted to assess previously introduced known movements. The results show that it possible to detect a movement with an accuracy of the order of 1.6 millimeters in real-time with a delay of just three minutes with excellent control over false alarms. The system was implemented in a real engineering project (the Pacoima Dam in California, USA) and it was shown that the method was able to detect deformations that are fully consistent with measured changes in the water surface level in the reservoir. The GPS data processing aspects of the software were verified by comparison of results with a commercial software (SKI-Pro) that uses a different methodology. In summary, an effective, low-cost approach for reliable engineering monitoring using GPS has been developed, and tested in controlled and real engineering environments.

. و بالرغم أن الGPS له بعض الأفضلية علي الطرق التقليدية في متابعة المنشات الهندسية إلا أنه لازال يعطي دقة لحظية منخفضة مما يعطل الاستخدام الامثل له في هذه التطبيقات. من أهم عوامل تدني الدقة في هذا النظام هو الخطأ الناتج من تأثير المسارات المتعددة لاشاراة الرصد (Multipath) . و يعتبر استخدام أسلوب (Sidereal-day correction) من انجح الطرق المستخدمة لتلافي هذا التأثير. وقد تم دمج الأسلوب مع ال Kalman Filter و احد مخططات ضبط الجودة للكشف عن أي تحركات لحظية في المنشأ الهندسي و ذلك عن طريق برنامج بالحاسب الآلي يدعي GPSEM . ومن اجل الحصول علي نظام منخفض التكاليف تم استخدام الأرصاد من الموجة L1 فقط. و قد تم اختبار هذا النظام و البرنامج علي العديد من التجارب الحقلية و كذلك علي منشأ هندسي قائم. وقد اظهرت النتائج من هذه التجارب مدي كفاءة كلا من النظام و البرنامج.

# High Accuracy Real-time Dam Monitoring Using Low-cost GPS Equipment

**Reda ALI, Paul CROSS, United Kingdom and Ali EL-SHARKAWY, Egypt**

## 1. INTRODUCTION

Many man-made and natural structures such as buildings, bridges, dams, and slopes undergo various forms of deformations. Precise monitoring of the progressive deformations of these structures can often provide vital information on the stability and safety status. It also provides valuable information used for calibrating design codes. There are many instruments that can be used for deformation monitoring, such as total stations, precise levels, and strain gouges. Although these instruments give reliable results, they suffer from many defects like, the effect of atmospheric refraction, the non applicability for all weather conditions and locations, and non suitability for real time applications. However engineers require an instrument that not only has a good accuracy, but also can overcome the shortcomings of the conventional methods.

Today the Global Positioning System (GPS) is so accurate that it makes sense to investigate if it can be used for engineering deformation monitoring at the millimetre level. GPS has provided a very useful tool for monitoring structural deformation, it offers may advantages over traditional surveying techniques that measure relative geometric quantities between selected points, and also over techniques that employ geo-technical instrumentation. In general, GPS is more accurate and efficient. It is highly automatic and not labour intensive. However, GPS also has its disadvantages when used for such applications. One limiting factor for large-scale use of GPS is its high cost. Another is the poor accuracy of GPS positioning in real time due to various types of systematic errors in certain engineering environments.

Most systematic errors are eliminated to some extent by using relative positioning techniques. The ultimate difficulty is to cope with multipath effects where the GPS signals reach to the antenna having been reflected from nearby surfaces. Multipath is the most limiting factor on accuracy for very precise positioning applications with GPS. It is very often present in construction and urban environments, and can amount to an error of few centimetres.

Unfortunately, the accuracy requirements of precision deformation monitoring are generally at the sub centimetre level, which is presently unachievable on an epoch-by-epoch basis with regular, carrier phase double difference techniques. Thus due to the multipath error not cancelled by the double differenced techniques, the multipath error is highly dependent on the environment around receiver. For individual GPS satellite Multipath influence is significantly correlated between subsequent days, because the satellite constellation repeats after a sidereal day, and thus Multipath geometry is very similar for a given station environment. Sidereal-day differences of GPS carrier phases are not as significantly influenced by multipath error as the original phase measurements due to the daily repetition of satellite positions [Wubbena et al. 1996]. Sidereal day differences of GPS carrier phases, are used for deformation analysis. Such differences have much less influenced by multipath errors than original phase measurements, due to the daily repetition of satellite positions.

This paper has focused on the implementation of the sidereal-day technique through software (GPSEM) that was developed at UCL to monitor an engineering object using single-frequency L1 phase GPS observation only. With the aid of Kalman filtering techniques and a Cumulative SUM (CUSUM) control chart, movements between two days can be extracted

from false movement due to multipath errors. Data from a real engineering object (dam in California, USA) is used for test the system and the software.

## 2. GPS CARRIER PHASE MULTIPATH ERROR

Multipath is the phenomenon whereby a signal arrives at a receiver via multiple paths due to reflection. Multipath distorts both the carrier and the code of GPS signal; the result is anomalous pseudorange and carrier phase measurements [Braasch 1992].

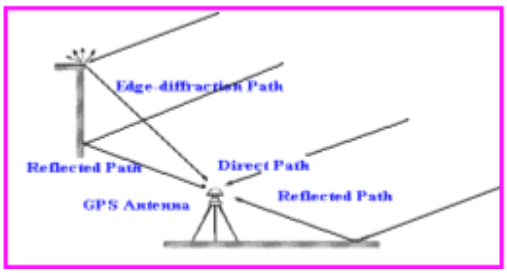


**Figure 1**: GPS Multipath

The multipath signal characteristics are a function of the satellite-reflector-antenna geometry, the multipath errors produced are more simply a function of the satellite elevation and azimuth with respect to user antenna. In other words, for a fixed reflector and stationary antenna; the multipath errors produced are more simply a function of satellite elevation and azimuth with respect to the user antenna. GPS satellite orbits are highly repeatable from day to day, thus multipath effects exhibit a day-to-day repeatability, and can therefore be removed by subtraction of appropriately stacked GPS results. The repeatability of multipath errors in stationary environments is well known and well documented [Georgiadou and Kleusberg 1988].

### 2.1 Sidereal-day Corrections Technique

Experiments carried out by [Ali 2003] show that The cross-correlation factor for double differenced L1 phase multipath errors between two days can reach to 0.89. This indicates the possibility of reducing the multipath impact in the recent data by using data from previous days. This technique is called the sidereal-day correction technique. Applying the sidereal-day correction technique improves the accuracy of multipath residuals for a certain double differenced pair by approximately 49% of the original accuracy. In other words the improvement factor could reach to two.

Applying the sidereal-day correction technique increases the noise in time series. On the other hand, it dramatically reduces the periodical nature of the multipath in original time series. So the noise in the final time series is more like white noise after applying sidereal-day correction technique, which makes the time series appropriate for the application of a filtering technique. Applying a one-minute moving average filter on L1 phase data after applying the sidereal-day correction technique improves the original raw time series of double differenced residuals by 60%. This indicates that promising results will be obtained if a more sophisticated filtering technique such as the Kalman filter is used.

Estimation of the time shift between two successive days is essential for carrying out sidereal-day corrections. An effective method for computing the time shift between two days based on searching for the nearest positions of a satellite in the sky between two days is

illustrated at[Ali 2003].The investigations carried out on the computation of time shift between two days using nearest satellite location show that there is a strong link between the computed correlation factors and the nearest distances of satellite locations between two days. Applying this method for computing the time shift gives an excellent quality control on data used for sidereal-day correction from any satellite. For example data from a satellite that has a large difference in its position between two days, is not used, or it is even dramatically down-weighted, when used in the sidereal-day correction technique.

## 3. GPSEM SOFTWARE FEATURES AND USED MATMATICAL MODELS

The software GPS Engineering Monitoring (GPSEM) is a program written in the C++ language that was developed at the Department of Geomatic Engineering, University College London (UCL). This software divides the processing of GPS data for Engineering Monitoring into two main parts:

- Initialization phase, which consists of the first 24 hour of data
- Continuously operating engineering monitoring phase.

### 3.1 GPSEM Initialization Phase

#### 3.1.1 Main Input Data

The main data required for GPSEM is navigation and observation files from the reference and rover stations. All the input files are in Receiver INdependent EXchange format (RINEX),it also require the coordinates of the reference station must be supplied in the WGS84 coordinates system; otherwise the program will use the approximated coordinates of the reference station derived from the navigation solution.

#### 3.1.2 Computing Satellites Parameters

This includes the satellites' positioning in WGS84 coordinates system, elevation angle and azimuth of each satellite. Also the satellite clock correction and radial velocity of the satellite.

#### 3.1.3 Initial Processing Steps

Three main steps are addressed: time tag synchronization, cycle clips detection and correction using normal point approach and applying troposphere correction of GPS observations using Mapping Function (NMF) [Neill 1996].

#### 3.1.4 Formation of Double Differenced Observation Equations

The reference satellite is usually chosen as the highest satellite in the sky in order to reduce the impact of outlying measurements (e.g. due to large multipath error) on the results. Formation of double differenced observation equation, normal matrix and variance covariance matrix.

#### 3.1.5 Solving for Integer Ambiguities and Cycle Slip Detection

This done using Fast Ambiguity Resolution Approach (FARA). A discrete Kalman filter used here to correct for any cycle slip and to estimate the new integer ambiguity associated with

each new rising satellite automatically. This technique is applied to the double differenced observation.

3.1.6 Output Files

There are two main outputs of GPSEM. The first is the position time series with the estimated accuracy of each computed position, and the second is a multipath estimation, which is essential for the next phase (monitoring phase). The first is denoted E_n_up which contain the observation time associated with three coordinates in the local coordinate system and the formal accuracy of these coordinates. While the second is denoted Multipath which contain all the necessary information enable the programme in its monitoring stage to reconstruct the time series of previous day. These data are stored in satellite base.

Figure (2) demonstrates the main parts of the GPSEM software during its initialization phase.

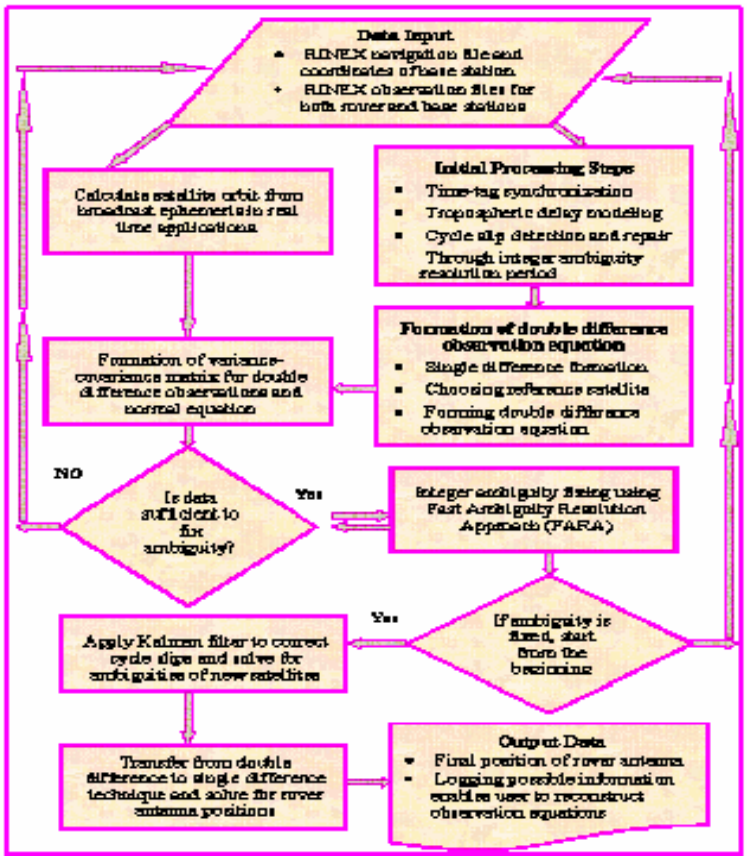


**Figure 2** : Data processing steps in GPSEM in its initialization phase

## 3.2 Continuously Operating Engineering Monitoring Phase

The initializing phase which lasts 24 hours to collect data used for correcting the multipath error in the successive day. The monitoring phase is using these data to detect the movement

and produce filtered time series coordinates. illustrates the processing steps in GPSEM software for engineering monitoring.

### 3.2.1 Estimate Sidereal Day Time Shift

Reliable estimation of sidereal-day time shift is an essential task to perform sidereal day correction. The used strategy through GPSEM is summarized as following:

- Kepler's third law of planetary motion is used to estimate an initial value for revolution period of slave satellite. This is simplified as

$$T = 2\left[2\pi\sqrt{\frac{r^3}{GM}}\right]$$

Where:

T is the sidereal-day time shift between two successive days
G is the universal gravitational constant
M is the mass of the Earth
r is the radius from the centre of the Earth to the centre of the satellite

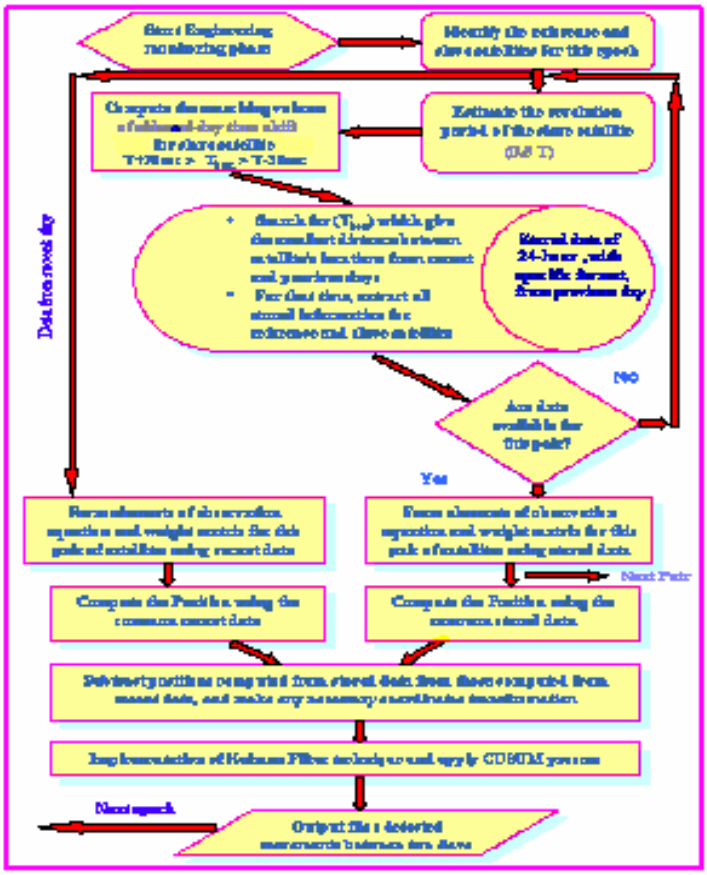

**Figure 3:** Data processing steps in GPSEM in its engineering monitoring phase

- The initial sidereal-day time shift computed from above equation is centred through a search volume with a width of 60 seconds. So the suggested sidereal-day time shift that will be used to perform sidereal day correction, is lie between two limits, the upper limit is T+30 seconds and the lower limit will be T-30 seconds.
- The coordinates of every slave satellite are individually used to search all available epoch that lies within the searching volume. The best-chosen epoch for this certain satellite is which giving the smallest distance between satellite's positions from recent and previous day. This is done by arranging the computed distance from this satellite at recent epoch to all its positions through the searching volume. If this satellite does not exist at the stored file, this satellite will not be used for any farther calculations, and it will be eliminated from the data of recent epoch.

3.2.2 Compute the Positions for Two Days

- The stored data for every satellite is formatted as in the following:
- Satellite identification number PRN
- Satellite position coordinate in X-direction in the WGS84 coordinate system
- Satellite position coordinate in Y-direction in the WGS84 coordinate system
- Satellite position coordinate in Z-direction in the WGS84 coordinate system
- Residual of single difference L1 phase observations with respect to the approximate coordinates of rover station.
- Number used in the stochastic model indicating the strength of signal

The approximate coordinates of the rover station are stated on the head of storing file and they are read immediately after the system transfer from initialization to engineering monitoring phase. To illustrate how the system works at this stage, it is better to give an example:

- Suppose we have for a certain epoch five double difference pairs with slave satellites PRNs 2, 3, 4, 5, and 6 with satellite PRN 1 as the reference satellite.
- After searching for the nearest location of satellite PRN2 through the suggested searching epochs on the stored file, all the information associated to this satellite, and reference satellite are extracted.
- Formation the elements of double difference design matrix using both coordinates of satellites 1, and 2 and the stored approximate coordinates of rover stations is carried out.
- The vector of double difference residuals is computed by subtracting the two values of single difference L1 phase .
- The process is continued for satellites PRN 3, 4, 5, and 6. If for any reason data from one of slave satellites does not exist in the previous day data, this double difference pair is then removed from data of the present epoch.
- After calculating the elements of design matrix and vector of double difference residuals the normal matrix is computed to perform the least squares solution. The only remaining problem is the construction of the weight matrix P. referee to [Ali 2003].

Following the above procedures, the positions of the rover station at an epoch in the previous day resembling those of the present epoch, where the satellite constellation is repeating itself, are computed. Computing the position for the present epoch does not contribute any complication, because the program is doing it continuously. The difference between two positions represents the movement that occurs between the two days. The time series of these

differences is nearly free of multipath, but contaminated with large amount of white noise, where the Kalman filter will have a vital job to play.

### 3.2.3 Kalman Filter Equations

The Kalman filter is defined by the following set of equations for the relevant least squares estimates and their covariance matrices as described in [Cross 1987]:

Time update (Prediction phase):

$$\hat{X}_{i}(-) = \phi_{i-1}\ \hat{X}_{i-1}$$

$$C_{\hat{X}_i(-)} = \phi_{i-1}\ C_{\hat{X}_i(+)}\ \phi_{i-1}^{T} + C_{y_{i-1}}$$

Measurement updating phase (Filtering phase):

$$G_i = C_{\hat{X}_i(-)}\ H_i^T \left[C_\ell + H_i\ C_{\hat{X}_i(-)}\ H_i^T\right]^{-1} \qquad \hat{V}_i(-) = b_i - H\ \hat{X}_i(-)$$

$$\hat{X}_i(+) = \hat{X}_i(-) + G_i\ \hat{V}_i(-)$$

$$C_{\hat{X}_i(+)} = \left[I - G_i A_i\right] C_{\hat{X}_i(-)}$$

Where

(-) , (+) is refer to instants immediately before and after measurement updates respectively.

$\hat{X}_{i-1}$ is least squares estimate of state vector.

$\phi_{i-1}$ is transition matrix from time i-1 to i.

$C_{\hat{X}_i}$ is covariance matrix of $\hat{X}_{i-1}$.

$C_{y_{i-1}}$ is dynamic model noise matrix for time i-1 to i.

$G_i$ is gain matrix.

$C_\ell$ is covariance matrix of observations at time i.

$I$ is the identity matrix

$b_i$ is vector of misclosure, (observed–computed) vector.

$H$ is design matrix of the measurement system.

$v_i$ is residuals vector (innovation sequence).

### 3.2.4 Adaptive Dynamic Models

The main problems faced by a dynamic model in a Kalman filter occur when the system experiences unexpected dynamic conditions, a change in data acquisition rate, or when in fact the dynamics of the system are non-linear. The more likely dynamic models which are implemented in Kalman filter through engineering monitoring, could be grouped as constant

velocity model, constant acceleration model and constant position model [Schwarz et al 1989]. Constant position and constant velocity model are the used models in this paper
In this case three positions and three velocities in east, north, and up respectively, represent the state vector. It is thus of the form

$$X^T = [E \quad N \quad UP \quad v_E \quad v_N \quad v_{UP}]^T$$

The corresponding transition matrix $\phi$ is of the form

$$\phi = \begin{bmatrix} I & \vdots & SD \\ \cdots & \cdots & \cdots \\ 0 & \vdots & T \end{bmatrix}$$

Where all sub-matrices are diagonal and have dimension (3*3). Their diagonal elements are of the form:

$$S = diag \{s\} = diag \{\alpha^{-1}(1 - t)\}$$
$$T = diag \{t\} = diag \{e^{-\alpha\Delta t}\}$$
$$D = diag \{d\} = diag \{1\}$$

The specific form of *T* indicates that corresponding elements of the state vector are modelled as first order Gauss-Markov processes satisfying a differential equation of the type

$$\dot{X} = -\alpha X + \omega$$

Where α is the inverse of the correlation length and $\omega$ is a white noise process. A large value of α i.e. a short correlation length, allows a large change of *X* from one measurement epoch to the next; a small value of α describes a strong correlation between subsequent measuring epochs and will thus give little variation in *X*. In that case, the transition matrix is well approximated by

$$\phi = \begin{bmatrix} I & \vdots & D \ \Delta t \\ \cdots & \cdots & \cdots \\ 0 & \vdots & T \end{bmatrix}$$

For constant $\Delta t$ the covariance matrix $C_y(\omega)$ corresponding to a constant velocity model can be modelled as:

$$C_y(\omega) = \begin{bmatrix} Q_1 \Delta t + D^2 S_{22} Q_2 & \vdots & D \ S_{23} Q_2 \\ \cdots & \cdots & \cdots \\ D \ S_{23} Q_2 & \vdots & S_{33} Q_2 \end{bmatrix}$$

$Q_1$ , and $Q_2$ are the uncertainties of first three and last three element of the state vector, respectively.
The *S*-matrices are diagonal and have diagonal elements of the form:

$$S_{22} = diag \{S_{22}\} = (-3 + 2\alpha\Delta t + 4 e^{-\alpha\Delta t} - e^{-2\alpha\Delta t}) / 2\alpha^3$$
$$S_{23} = S_{32} = diag \{S_{32}\} = (1 - 2 e^{-\alpha\Delta t} + e^{-2\alpha\Delta t}) / 2\alpha^2$$
$$S_{33} = diag \{S_{33}\} = (1 - e^{-2\alpha\Delta t}) / 2\alpha$$

If α is very small due to large correlation length $C_y(\omega)$ can become approximated by:

$$C_y(\omega) = \begin{bmatrix} Q_1 \Delta t + \frac{D^2}{3} Q_2 \Delta t^3 & \vdots & \frac{D}{2} Q_2 \Delta t^2 \\ \cdots & \cdots & \cdots \\ \frac{D}{2} Q_2 \Delta t^2 & \vdots & Q_2 \Delta t \end{bmatrix}$$

The constant velocity model is set to be the default mode in this study by setting the correlation time very large. In this investigation we expect that there is no deformation in the monitored engineering object, so a constant position model is considered, and the residuals of the Kalman filter are continuously monitored. If there is a deviation in the residuals, the model is adapted to be a constant velocity model. The constant velocity model is set in the mode of constant position by setting the inverse of the correlation length α to be very large. This effectively sets the values of *S* to zero. when the filter detects an error in the dynamic model, through the innovation sequence, the α value are reduced to give the constant velocity model.

3.2.4 CUmulative SUM (CUSUM) Chart

CUmulative SUM (CUSUM) chart, where the information from successive readings, are cumulated to form CUSUM chart. The CUSUM control charts were first proposed by Page 1954 and have been studied by many authors. CUSUM chart is used here to monitor the innovation sequence of the Kalman filter output under some decision criteria, if the filter divert its suggested state the CUSUM will sound an alarm and switch to another dynamic model. The CUSUM chart starts out at its initial state. Each episode of positive values will end in one of two ways: either the CUSUM returns to zero, or it crosses the decision interval. When the chart crosses the decision interval, this indicates that a shift has occurred and actions will be taken to diagnose the shift. Generally the CUSUM will then be restarted. The number of observations from the starting point up to the point which the decision interval is crossed is called the run length. interested reader advised to refer to [Montgomery 2001].

## 4. CONTINOUSLY MONITORING PACOIMA DAM USING GPS

Located in Pacoima Canyon in the San Fernando Valley, California, USA, the Pacoima concrete arch dam was completed in 1929, measuring 372 feet high and 640 feet wide, and is still in operation. At its completed construction date, it was considered to be the tallest dam in the world. It's one of 15 dams run and maintained by Los Angeles County, and it locates on Pacoima Wash, which is one of eight major tributaries to the Los Angeles River as it flows from its headwaters to the Pacific Ocean. Figure (4) shows the location of the Pacoima dam.

The two points (DAM1 and DAM 2) on the dam were instrumented with dual frequency P-code GPS receivers and incorporated into the Los Angeles Basin's dense GPS geodetic array. The design of this system and its communications and operations are based directly on that of the permanent GPS geodetic array that was the forerunner of the Southern California Integrated GPS Network (SCIGN).

**Figure 4** : Pacoima dam view

The two points (DAM1 and DAM 2) on the dam were instrumented with dual frequency P-code GPS receivers and incorporated into the Los Angeles Basin's dense GPS geodetic array. The design of this system and its communications and operations are based directly on that of the permanent GPS geodetic array that was the forerunner of the Southern California Integrated GPS Network (SCIGN).

Station DAM1 was installed on roof of a single-story, concrete operations building on south thrust block of the dam, station DAM2 was installed near the centre of the dam arch, these stations form a 103.7 metres baseline differing in height by only 0.66 metres. Figure (5) shows the location of both two stations, and their associated equipment.

SCIGN has coordinated the design and assembly of the deformation monitoring system of Pacoima Dam. Like any GPS deformation monitoring system every station should consist mainly of five components: GPS receiver, Radio modem, GPS antenna, monument, and power supply. Both stations are equipped with Ashtech Z-XII3 GPS dual frequency receivers; the elevation cut-off angles are setting to be 10 degree in both stations.

DAM1 DAM2

**Figure 5** : Stations DAM1 and DAM2 on Pacoima Dam

Two Ashtech 700936A_M Choke Ring with radome antennas in both base station (DAM1), and rover station (DAM2). The antenna at the base station was attached to a threaded rock pin; the pin is set in roof of dam house on concrete abutment. While at the rover station, the antenna is attached to top of a specially built pier that approximately 2 metres tall so as to put the antenna above height of chain link fencing that runs the length of the dam crest. The power is supplied to both stations from the dam house and all equipment are protected inside a metal box, hanging on the fence at station DAM2, or on the dam house building.

### 4.1 Previous Studies on Monitoring Pacoima Dam Using GPS

[Behr et al 1998] describe the initial 2 years of operation and observations for this system. The highlight of that analysis was the identification of an oscillatory displacement of DAM2 station of approximately 17 mm peak-to-peak amplitude with respect to DAM1 with an approximately annual period. This analysis showed that this displacement was strongly related to the air temperature surrounding the dam.

In [Hudnut and Behr 1998] the analysis was extended to cover all data from 1 September 1995 to 26 July 1998 using quarter day solution with sophisticated spectral analysis of the residual time series. This study indicates strong coherence at frequencies as high as 1 cycle per 14 days between remotely recorded temperature and dam displacement. On other way they can able to derive and apply an impulse response function between input temperature and output displacement that enable a resolution of 2-4 mm displacement over a periods of a few days. The residual deformation record could be used to model the structure's response to change in reservoir level and identify anomalous displacements at Pacoima dam.

In this paper we concentrate only on the response of the dam under changes of water level in the reservoir during flood periods, as the change in temperature between two successive days is relatively small and its effect on dam movements is negligible.

### 4.2 Data Availability and Processing Strategy

The data for both GPS points DAM1, and DAM2 (Navigation and observation RINEX Format files) are available through the SCIGN web site location [SCIGN web site] from September 1995 to Mach 2000. Data from DAM1 was installed from 03/08/1995 and the station was decommissioned on 4 April, 2000 due to new construction at the site, so the last day of data was in 28/03/2000, a new station was installed called DAM3, unfortunately, data from this station are not available from the SCIGN web site. The observation rate of these data is 1/30 Hz, and the mask angle for the original raw observations was chosen to be 5o. Actually the mask angle is chosen to be $15^{o}$ in the GPSEM to reduce the impact of signal diffraction on the data.

The present system at Pacoima Dam does not operate in real-time because of existing limitations in telemetry and data processing capabilities. Many manufacturers of GPS equipment now offer real-time systems that can make measurements of centimetre-level precision at rates exceeding 1 Hz. Such systems were experimental when Pacoima Dam was instrumented with GPS in September 1995 and are still relatively costly to implement today. But the program operates as if the data are processed in real-time

The dam deformation is not monitored by any conventional method. This makes the assessment of the system's accuracy difficult. The precision of the system under similar conditions such as water level and temperature is studied. The orientation of the dam body is approximately the same as the line joint the two points DAM1 and DAM2. This makes the azimuth of the principle axis of deformation equal approximately 296$^{o}$.

### 4.3 Pacoima Dam Water Level Data

The Water Surface Elevation was read from a guage boarded in the dam's reservoir and it is marked in tenths of a foot. The department of public work, Los Angeles County, provides these data. Figure (6) graphs part of water level data for a minor flood period.

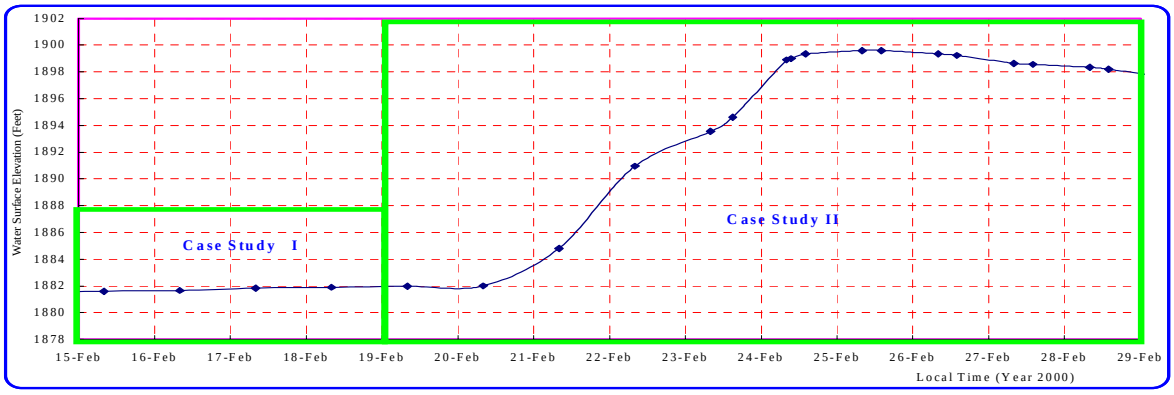


**Figure 6** : Water surface elevation in Pacoima Dam's reservoir

As is obvious from this figure the analyses of dam deformation under water pressure are divided into two parts: the first is used to access the precision of the system and the second is used to investigate the behaviour of the system under loads introduced from water level variations.

### 4.4 Analyses on the First Case Study

Data from four sequences days are processed using GPSEM. The time series of the coordinates in the three directions (i.e. along deformation axis, perpendicular to deformation axis) are plotted against GPS time for the four days; figure (7 ) shows this time series.

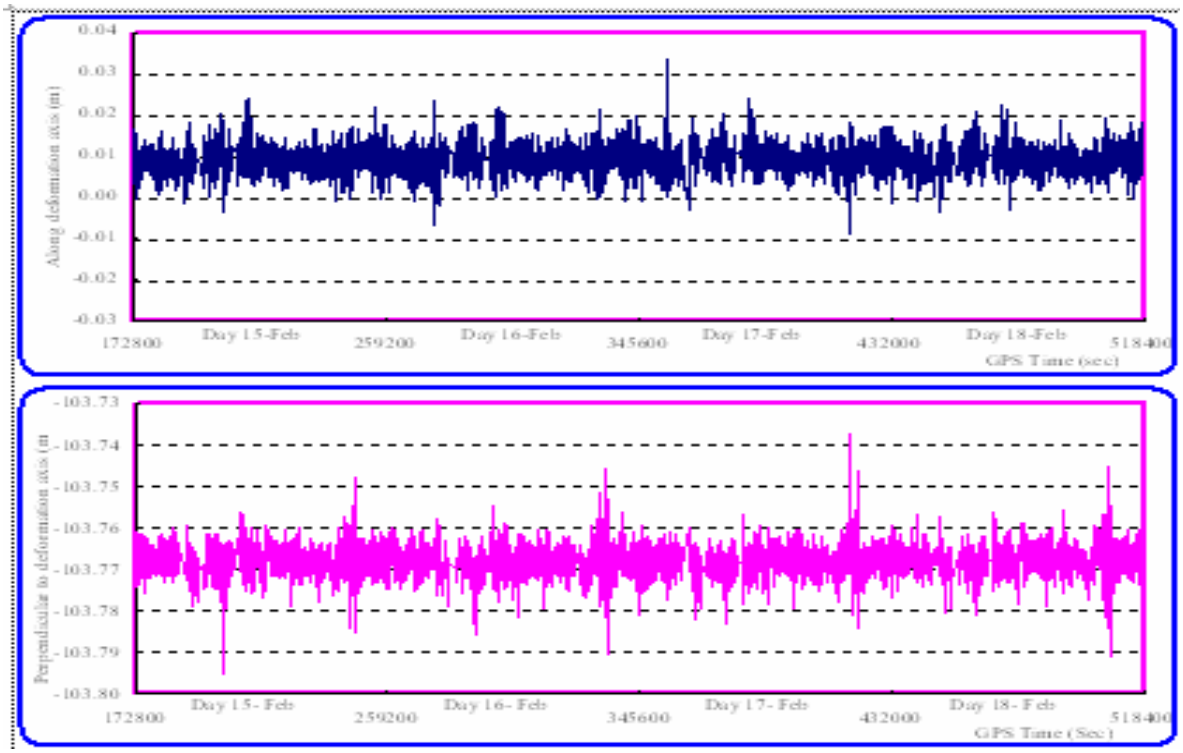


**Figure 7 :** Time series of coordinates for the four sequenced days

4.4.1 Applying Sidereal day Corrections and Kalman Filter

Figure (8) shows the deformation of the dam in the along deformation axis, perpendicular to the deformation axis respectively. These deformations are computed using the sidereal-day corrections technique and then filtered using Kalman filter using GPSEM.

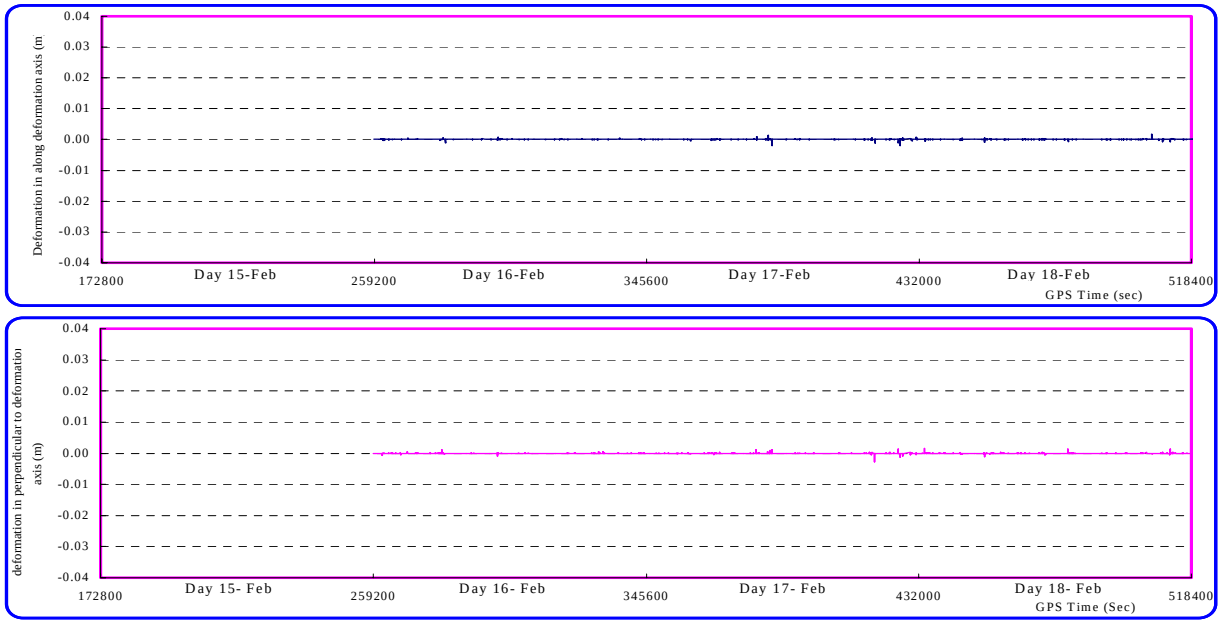


**Figure 8:** Filtered deformation occurred between the four days

As seen from figure (8), there is no data (i.e. deformation) for day 15-Feb. as the data from this day is taken as reference. In other words, the data shown for day 16-Feb. represent the deformation that occurred between days 15 and 16 February 2000, and those of day 17-Feb. represent the difference in deformation between day 16 and 17 Feb., and so on.

4.4.2 System Precision Assessment

To assess the precision of the system, we shall look at the behaviour of the system from day to day, and also the factors that cause these movements between the two days. The system is said to be precise if it reacts in the same way under similar conditions.

The two possible factors that can cause dam deformation are: an increase in water level in the dam reservoir or change in temperature. As seen from the figure (6) the difference in water levels between two successive days is in order of 0.1 feet (i.e. ≈ 3.4 cm). This tiny change in water level will not cause any significant change in the water pressure on the dam, which in turn has no impact on the dam deformation.

The second factor is the temperature change between two days. It worth here to state that, the temperature mentioned should be the temperature of the dam core. The dam core temperature sensors were removed from the structure shortly after the Northridge earthquake, so there is no observations taken for dam itself. The only available information is the metrological data collected at DAM2 point, and the dam will take long period of time to respond to large change in temperature. These data are used to plot the recorded temperature around the dam and the difference between two successive days on the same GPS time scale.

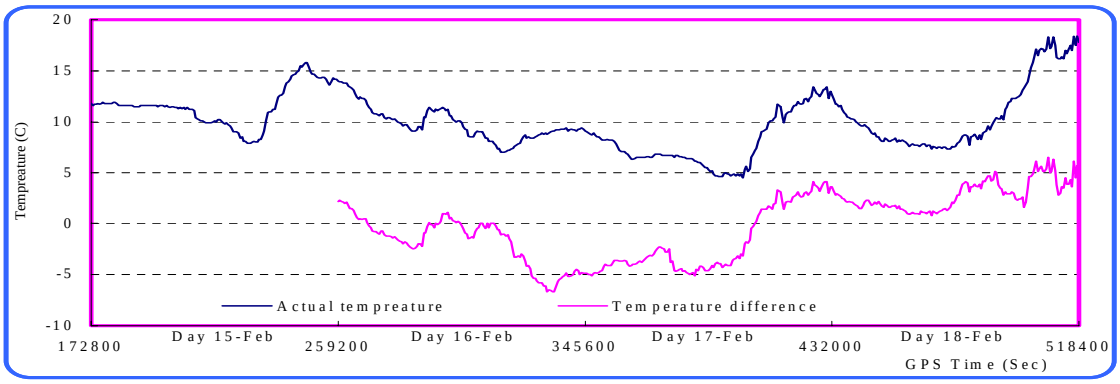


**Figure 9 :** Actual temperature and temperature variation between two successive days

It obvious from figure (9) that the average of the differences in temperatures between two successive days are in order of $2^{o}$ C. The effect of these differences on dam deformation is negligible. So the drawn conclusion from (6), and (9) is that there is no cause for any movements to occur between any two successive days, the question now is: does the output from the program reflect this reality?

From statistical analyses of time series for the four days and figures (8) the following conclusions have been drawn:

- The analysis of time series of raw coordinates shows that, there is no significant change in the mean between two successive days, the maximum change is in order to 0.3 mm in

along deformation axis and 0.6 mm in UP direction. This gives a clear indication of there is no movements occurred between any two successive days. The times series of coordinates after applying sidereal-day corrections shows similar values, in addition, their standard deviations are reduced dramatically.

- After full implementations of the technique (i.e. sidereal day correction, Kalman filter, and CUSUM), the results show no deformation is detected with high precision in real-time. The standard deviations of the time series are in order of ±0.1 mm.
- It can clearly be seen that the behaviour of the dam from day to day is consistent with the Geotecnical measurements within ±0.04 mm. This confirms that, high precision can be obtained by applying the proposed system in such deformation monitoring applications.

### 4.5 Analyses on the Second Case Study

The same procedures mentioned in section (4.4) are used in the analysis of time series of the coordinates from day 19-February to day 28-February, 2000. Figure (10) illustrates the raw time series of coordinates for ten successive days.

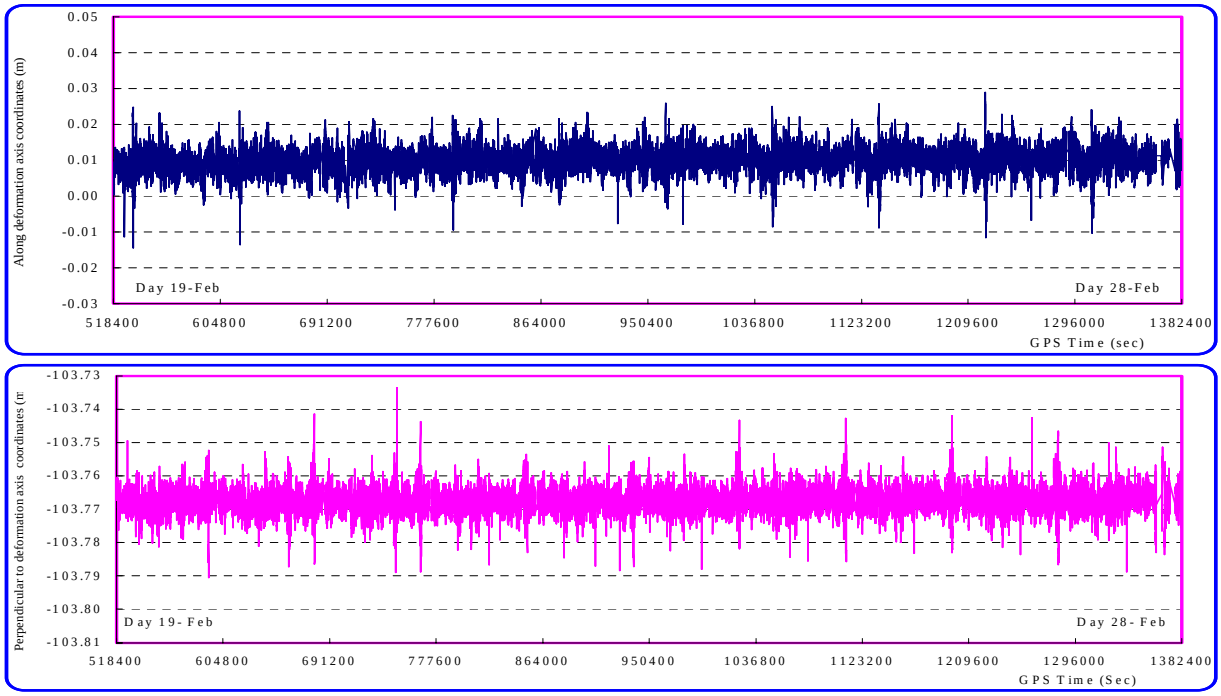


**Figure 10**: Time series of coordinates for the ten sequenced days

It appears from the top part of figure (10) that there is a periodical deformation, but the Fourier analysis of this time series as shown in figure (11) enables a better interpretation. It shows that the data are dominated by signals with peak amplitude occurring harmonically every sidereal day. The most likely cause of this periodical nature is a multipath error. It is also obvious from the Fourier analysis that, there is a signal that has a period of approximately 24 hours.

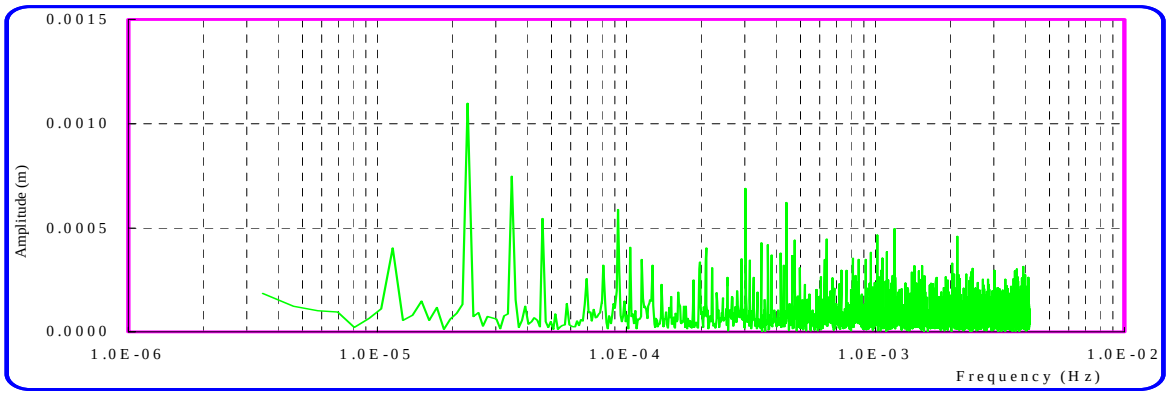


**Figure11:** Fourier analysis of time series of along deformation axis (top part of figure11)

The figure (12) plots the deformation in the along deformation axis, and perpendicular to the deformation axis against the GPS time for the ten days after applying sidereal-day corrections

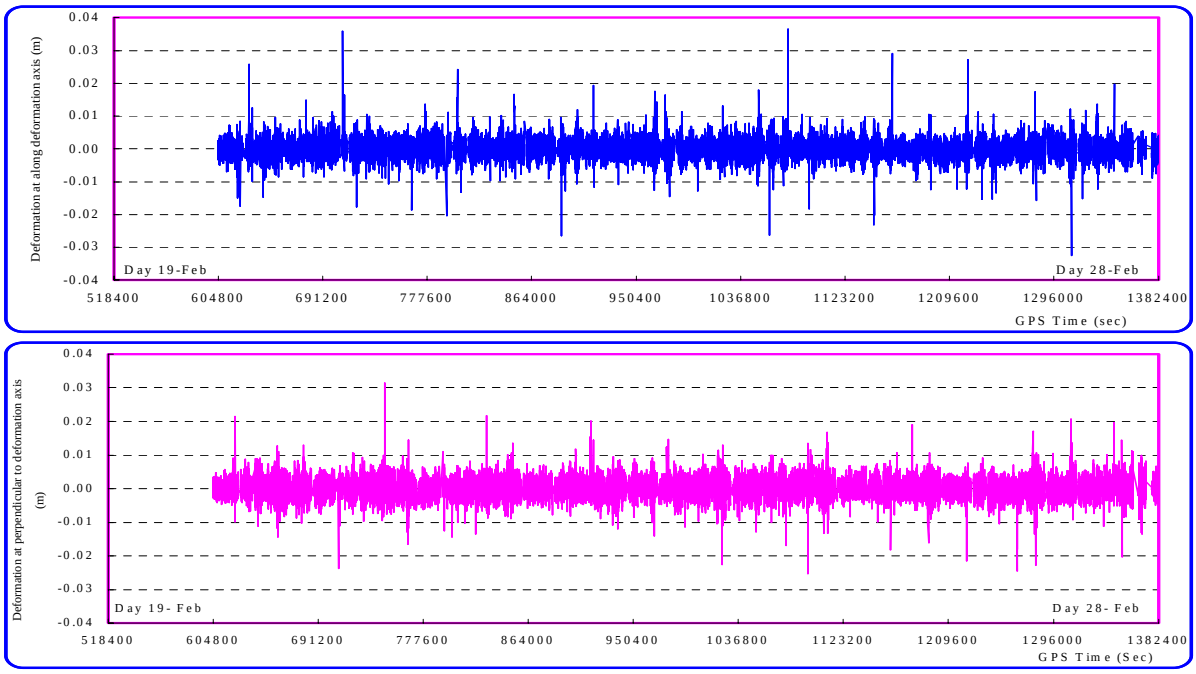


**Figure 12:** Dam's deformation after applying sidereal-day corrections technique

- It can be seen that the periodical nature is no longer apparent. If the data shown in figure () is filtered, the result will only be the deformation that occurred between the two successive days. To overcome this, the following procedures are adopted to enable GPSEM to work continuously:
- The deformations are considered to be zero on the first day (i.e. the first day is taken as a reference) and stored in a file.

- For any recent epoch, the computed deformation values are added to those in the file (at the appropriate sidereal time).
- The process is carried out for the next epoch, and so on till the end. In other words, the output will be an accumulated time series of the filtered deformation.

The dam's deformations are plotted for the ten days as shown in figure (13), which represents the final output of GPSEM with respect to deformation of day 19 February as a reference.

4.5.1 Deformation Consistency with the Water Surface Elevation

From figures (13) and figure (6) it seen that, there is a strong correlation (≈ 98%) between the deformation occurred along principle deformation axis and the water surface level in the reservoir. This indicates that the dam responds to change in the water pressure and so validates the operation of GPSEM. In order to further validation for GPSEM the LEICA SKI-Pro GPS software is used to process the data for whole 24-hour to overcome the problem of multipath error. The output is the three coordinates in WGS84. These coordinates are transformed to bring these coordinates in the same frame. Figure (14) shows the deformations at the along deformation axis direction computed from the SKI-Pro GPS software. These deformations are computed with respect to deformation of day 19 February which is taken as a reference.

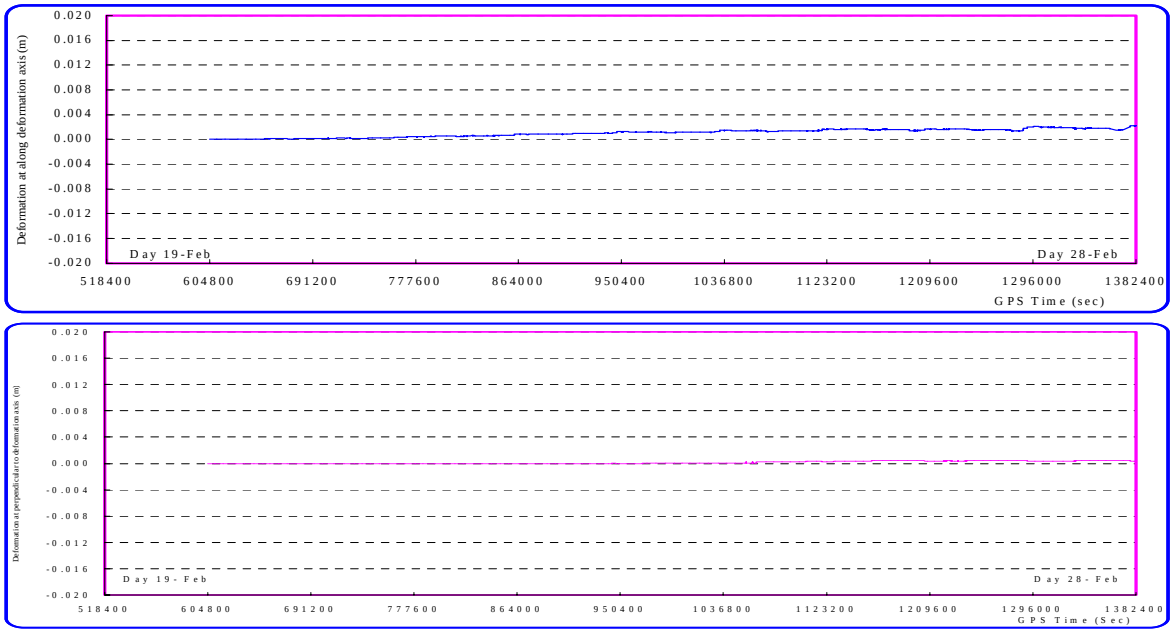


**Figure 13:** Accumulative filtered deformation occurred from days 19 to 28 February 2000

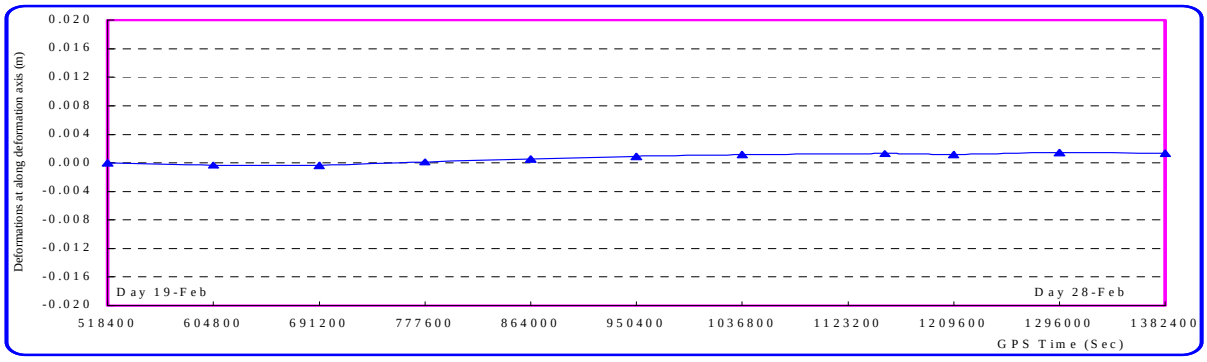


**Figure 14 :** Dam's deformations computed from SKI-Pro GPS software

The RMS of the differences between the two solutions (i.e. SKI-Pro and GPSEM) is ± 0.43 mm.

## 5. CONCLUSIONS AND RECOMMENDATIONS

Based on the results obtained from the investigations carried out on Pacoima, The system shows high precision for detecting deformation of a real continuous monitoring GPS project, and there is a strong correlation (≈ 98%) between the deformation occurred along principle deformation axis computed from the GPSEM and the water surface level in the reservoir. The dam's deformations computed from GPSEM in real time show high consistency with those computed from commercial software (i.e. SKI-Pro) using 24-hour solution. The RMS of the differences between the two solutions is ± 0.43 mm.
The suggested technique shows excellent results in GPS engineering monitoring applications that have low amplitude and frequency movements such as dams, regulators, locks, earth slope, building and short-span bridges. More investigations are needed to study the behaviour of the technique under high amplitude and frequency deformation that may occur in long-span bridges for example.

## REFERENCES

1. Ali Reda (2003)" High accuracy real time engineering monitoring using low cost GPS equipment" PhD thesis under joint supervision of Helwan university and University College London (UCL), Cairo, Egypt.
2. Behr, J., Hudnut, K., and King, N., (1998) "Monitoring Structural Deformation at Pacoima Dam, California Using Continuous GPS." Proceedings of the 11th International Technical Meeting of the Satellite Division of the Institute of Navigation [ION GPS-98], Nashville, TN, USA, 15 -18 September, PP. 59-68.
3. Braasch, M., (1992) "Characterization of GPS Multipath Errors in the Final Approach Environment." Proceedings of Fifth International Technical Meeting of The Satellite

Division of the Institute of Navigation (ION GPS-92), Albuquerque, NM, USA, 16-18, September, PP. 383-394.

4. Cross, P., (1987) "Kalman Filter / Smoother Equations: Their Derivation and Implementation." Paper Presented at the Royal Institution of Chartered Surveyors / Hydrographic Society Seminar on Kalman Filtering, University of Nottingham, 4 February.
5. Georgiadou, Y., and Kleusberg, A., (1988), "On Carrier Signal Multipath Effects in Relative GPS Positioning." Manuscripta Geodaetica, Vol. 13(3), PP. 172-179.
6. Hudnut, K. W. and J. A. Behr, Continuous GPS Monitoring of Structural Deformation at Pacoima Dam, California, Seis. Res. Lett., vol. 69, No. 4, pp. 299-308, 1998.
7. Montgomery, D., (2001). "Introduction to Statistical Quality Control", Fourth Edition, John Wiley & Sons, Inc., New York, USA, 796 P.
8. Niell, A. E., (1996), "Global mapping functions for the atmosphere delay at radio wavelengths." Journal of Geophysical Research, Vol. 101(B/2), PP. 3227-3246.
9. Wubbena, G., Schmitz, M., Menge, F., Seeber, G., and Volksen, C.,(1996) "A New Approach for Field Calibration of Absolute Antenna Phase Centre Variations." 9th International Technical Meeting of the Satellite Division of the Institute of Navigation (ION GPS-96), Kansas City, Missouri, USA, 17-20 September, PP.1205-1214.

## CONTACTS

Reda Mohamed A. Ali
Lecturer at Civil Engineering Department Faculty of Engineering
Helwan University Egypt
P.O. Box 11718 masaken Elhelmia
Cairo
EGYPT
Tel. + 20 13 2512 405
Mobile +20 10 6740066
Fax +20 24 156505
Email: redamaa@hotmail.com